Design and Analysis of a Two-winding Wireless Power Transfer System With Higher System Efficiency and Maximum Load Power

line 1: 1st Given Name Surname
line 2: *dept. name of organization*
(of Affiliation)
line 3: *name of organization*
(of Affiliation)
line 4: City, Country
line 5: email address or ORCID

line 1: 2nd Given Name Surname
line 2: *dept. name of organization*
(of Affiliation)
line 3: *name of organization*
(of Affiliation)
line 4: City, Country
line 5: email address or ORCID

line 1: 3rd Given Name Surname
line 2: *dept. name of organization*
(of Affiliation)
line 3: *name of organization*
(of Affiliation)
line 4: City, Country
line 5: email address or ORCID

line 1: 4th Given Name Surname
line 2: *dept. name of organization*
(of Affiliation)
line 3: *name of organization*
(of Affiliation)
line 4: City, Country
line 5: email address or ORCID

line 1: 5th Given Name Surname
line 2: *dept. name of organization*
(of Affiliation)
line 3: *name of organization*
(of Affiliation)
line 4: City, Country
line 5: email address or ORCID

line 1: 6th Given Name Surname
line 2: *dept. name of organization*
(of Affiliation)
line 3: *name of organization*
(of Affiliation)
line 4: City, Country
line 5: email address or ORCID

Abstract— **Wireless Power Transfer (WPT) system requires the two major modeling aspects comprising of maximum load power and high system performance. This paper analyses the concept used to assess the maximum output power and high system efficiency under varying coil separation, various working frequencies with dynamic load conditions through a conventional two-coil WPT system. Besides developing analytical links between load power and system performance, a developer can select an optimum design for the enhancement of the WPT system. A demonstration of the circuit model has been built in MATLAB/SIMULINK to examine the system's efficiency and output power. The obtained data are shown to be in close agreement with the relevant operating principle and offer results for the simulation prototype based on the various functioning criteria mentioned above.**

Keywords— Wireless power transfer, highest system efficiency, maximum load power, frequency, separation, load

I. INTRODUCTION

Electric vehicles (EVs) driven by batteries are now an efficient alternative to the energy loss and pollution generated by internal combustion engines [1]. EVs are estimated to account for 30% of the latest car industry by 2030, having a yearly expansion rate of 44 million [2]. EVs, on the other hand, are not widely accepted due to various worries about the charging procedure and battery autonomy. Wireless power transmission resolves such challenges by providing charging more customer-friendly and enabling in-motion charging of batteries [3–4].

The wireless EV charging station seen in Figure 1 is a typical example. It is composed of a number of techniques for wirelessly charging an electric vehicle [5-6]. Initially, alternating energy from the grid is converted into direct voltage via a power factor adjusted alternating current to direct current converter. A compensated circuit is used to convert the direct current power to a high-frequency alternating current, which is then used to power the transmitting coil.

The high-frequency current in the transmitting coil creates an alternating magnetic field, which causes an alternating current voltage to be induced on the receiving coil. The transmitted power and efficiency are largely boosted by resonating with the secondary compensating circuit. Finally, the alternating energy is rectified in order to charge the battery.

WPT typically incorporates a significant gap between the primary and secondary coils [7-8]. As a result, the electric properties of the transformers utilized differ greatly from those of ordinary transformers with good winding coupling. WPT has a comparatively significant leakage inductance, as well as enhanced proximity-effect and winding resistances, due to the considerable winding spacing. Furthermore, in a WPT system with an air gap between the main and secondary windings, the magnetizing flux is greatly decreased. As a result, a greater magnetizing current is required, as well as circuit compensation for the larger leakage inductances.

Several procedures, including as frequency tuning, impedance matching, and design modification, have been proposed to produce the highest possible output power or to optimize system performance [9-11]. When compared to other ways, frequency tuning is one that might track split frequencies in the coupling region in order to obtain improved conversion efficiency and maximum load power. As a result of changes in coupling variables and mutual inductance in various distance conditions or imperfect coupling, impedance matching becomes an additional option for increasing process efficiency as well as load power [11]. This is accomplished by compensating for impedance malfunction caused by changes in coupling variables and mutual inductance in various distance conditions or imperfect coupling.

In a WPT system, the bifurcation phenomena describe a condition in which the frequency required to produce a zero-phase angle (ZPA) is not unique [12-13]. The number of frequency points required to implement a ZPA is determined by the dynamic loading, compensating schemes, and capacitor sizes. To ensure system reliability, this bifurcation behaviour, which is associated with numerous loading and variable frequency control, can be minimized.

The study discusses the design of a two-winding WPT system, which is used to achieve the best efficiency of the

system as well as the highest load power under a variety of coil separations, operating frequencies, and load conditions. Section II describes the WPT system's design information and analyses how to get the best overall performance while also delivering the highest possible load power. Section III presents and discusses simulated data, while Section IV summarizes the conclusions of the study.

II. DESIGN AND ANALYSIS OF THE WPT SYSTEM

A. Working Frequency

The working frequency of an ICPT technology is a vital aspect of its development. The power that can be transmitted through an IPT system is linked to the working frequency. Greater working frequencies, on the other hand, provide potential challenges for the power electronics operating the IPT system, as they can result in greater switching losses, ferrite losses, and possibly high powering voltages for the coils owing to coil inductance. Earlier IPT systems typically worked at a frequency of about 20 kHz. In the current scenario, due to advancement of Power electronic converter, the typical frequency range for EVs charging is 79-90 kHz as per the SAE stander report J2954 in [14]. For this paper, the operating frequency 85 kHz was considered at resonance frequency for this system. Although SAE J2954 addresses components with a maximum power rating of 22 kW (with higher power component standards currently conditionally specified), the same 85 kHz frequency is used here for compatibility with today's regulations.

B. Circuit Analysis

The schematic representation of the conventional wireless power transfer (WPT) structure involves a DC excitation, a high-frequency inverter, transmitter and receiver coils, high-frequency rectifier and a DC output is depicted in Fig. 1. Fig. 2(a) and 2(b) present the modified circuit and the equivalent circuit models of a two-winding WPT system, in which M depicts a mutual inductor described in equation (1); k denotes coupling coefficient; R_s is the internal resistance of the excitation; L_t and L_r denote self-inductances of the transmitter and receiver coils.
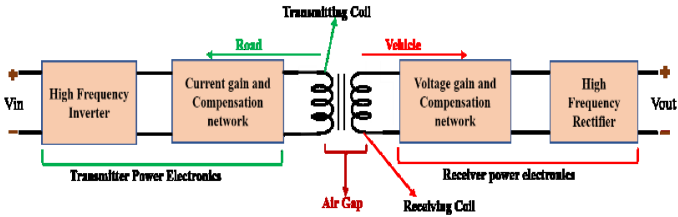
Fig. 1.   Schematic representation of a two-winding ICPT system

$$M = k\sqrt{L_t L_r} \qquad (1)$$

$$f_o = \frac{1}{2\pi\sqrt{LC}} \qquad (2)$$

(a)

(b)

Fig. 2.   (a)Two winding WPT structure (b) equivalent circuit referred to transmitting side

Equation (2) provides the transmitter and receiver coils frequency of self-resonance, in which L and C denotes the inductance and capacitance, individually. The impedance of the equivalent circuit has been defined by equation (3) and (4) and its corresponding KVL equation in (5)[9]. The ratio of load voltage to the input voltage defines the gain of the system, is described in the equation (6) as well as the transmitter and receiver currents are provided by equation (7) and (8), respectively.

$$Z_t = R_s + R_t + j\omega L_t + \frac{1}{j\omega C_t} \qquad (3)$$

$$Z_r = R_L + R_r + j\omega L_r + \frac{1}{j\omega C_r} \qquad (4)$$

$$\begin{bmatrix} Z_t & -j\omega M \\ -j\omega M & Z_r \end{bmatrix} \begin{bmatrix} I_1 \\ I_2 \end{bmatrix} = \begin{bmatrix} V_s \\ 0 \end{bmatrix} \qquad (5)$$

$$V_G = \frac{V_L}{V_s} = \frac{j\omega M R_L}{Z_t(Z_r+R_L)+\omega^2 M^2} = \frac{j\omega k\sqrt{L_t L_r}R_L}{Z_t(Z_r+R_L)+\omega^2 k^2 L_t L_r} \qquad (6)$$

$$I_1 = \frac{Z_r V_s}{Z_t Z_r+\omega^2 M^2} \qquad (7)$$

$$I_2 = \frac{j\omega M V_s}{Z_t Z_r+\omega^2 M^2} \qquad (8)$$

The magnitude and phase plot of V_G for the two winding ICPT system incorporating MATLAB/SIMULINK responses are depicted in Fig. 3, depending upon the specifications illustrated in Table I. The coupling coefficient between a transmitter to receiver coil has been $k = 0.25$. Fig. 3 demonstrates the effect of the simulation built on its developed model well correspond to the estimated gain and the phase points. The phase deviation in the position of transmitter and receiver coils is $\pi/2$ at the resonant frequency of 85 kHz.

TABLE I.   COMPONENT DESCRIPTIONS OF THE ICPT SYSTEM

Components	Values	Components	Values
R_S	1 Ω	R_L	6.34 Ω
L_t	120µH	L_r	120µH
C_t	29.28nF	C_r	29.28nF
R_t	0.5Ω	R_r	0.5Ω
k	0.01-0.25	f_o	85KHz

(a)

(b)
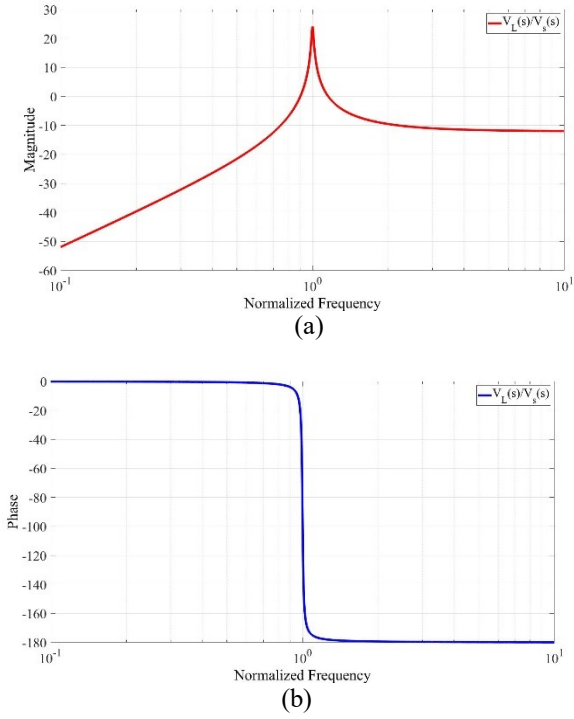
Fig. 3.   Bode plot of V_G at k=0.25 (a) Magnitude plot (b) Phase plot

Derived from the two-coil WPT device structure given in Fig. 2, system performance as well as load power should be determined in accordance with (9) and (11)[7].

$$\eta = \frac{P_{out}}{P_{in}} = \frac{Real\{Z_t'\}}{R_S+R_t+Real\{Z_t'\}} \times \frac{R_L}{R_S+R_t} \qquad (9)$$

in which $Real\{Z_t'\}$ denotes the real part of the impedance Z_t' depicted in the Fig. 2(b) and described as,

$$Real\{Z_t'\} = \frac{(\omega M)^2(R_S+R_t)}{(R_S+R_t)^2+\left(\omega L_t-\frac{1}{\omega C_t}\right)^2} \qquad (10)$$

$$P_{out} = \left|I_2^2 . R_L\right| = \left|(\frac{j\omega M V_s}{Z_t Z_r+\omega^2 M^2})^2 \cdot R_L\right| (11)$$

The WPT system performance of efficiency and load power with respect to normalized frequency at three distinct coupling coefficient such as k_1=0.08, k_2=0.17, k_3=0.25 are shown in Fig. 4. It is shown in the Fig. 4(a), that the highest system efficiency occurs at operating frequency for above respective coupling coefficients, whereas seen in Fig. 4(b) the load power changes over normalized frequency, as well as the high coupling variable is linked with two peak values. The highest overall output improves for the operating frequency with increasing k (separation between the coils reduces) as seen from fig. 4(a). The overall efficiency, as instance, reaches just 90% if k = 0.08, and when k becomes 0.25, it improves over 97%.

(a)

(b)

Fig. 4.   (a) System efficiency versus Normalized frequencies (b) Normalized load power versus Normalized frequencies
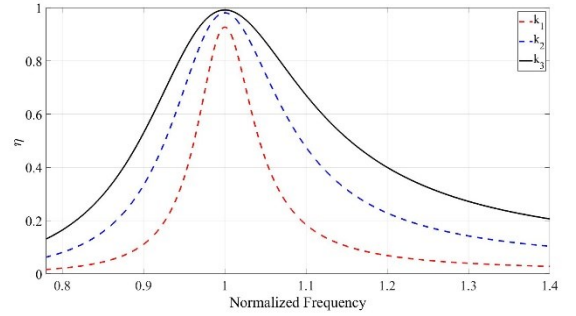
From the Fig. 4(b), the efficiency for 85 kHz operating frequency is just no longer the best value when k goes up. For this situation, a bifurcation of the frequency appears that deteriorates the transmitted power. At k= 0.08, for instance, two separate spikes become f_1 81802 Hz and f_3 88647 KHz.

For f_o=85 KHz, normalized power output falls around 73 %. This is why higher load power could be achieved through adjusting frequency relying to specific coupling coefficients (for several coil separations and misalignment conditions).

The performance of the system and load power can be seen in Fig. 5 as per the coupling coefficient including three distinct
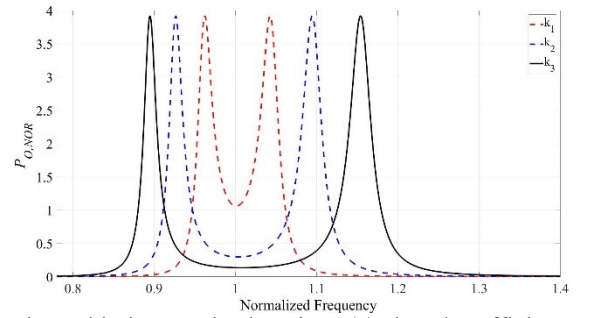
frequencies. This is seen in the Fig. 5(a) that the efficiency reduces eventually although the coupling coefficient drops. Moreover, at 85 KHz operating frequency, efficiency becomes more than that of as f_1 is 81802 KHz and f_3 is 88647

KHz.

(b)
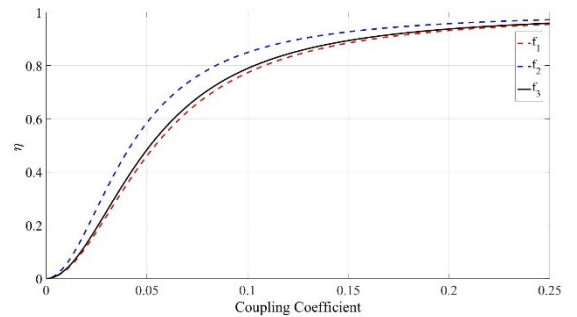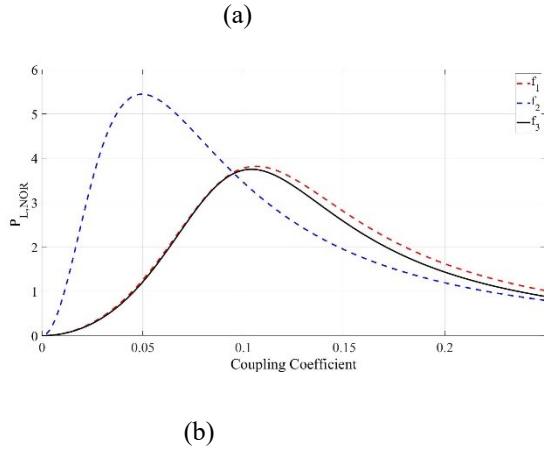
Fig. 5. (a) System efficiency versus various Coupling Coefficients (b) Normalized load power versus various Coupling Coefficients

Fig. 5(b) shows that load power firstly goes up and thereafter significantly falls. The highest possible load power value for f = 85 KHz appears with a reduced coupling factor value (k = 0.08), that means more power could be transmitted from the system at a higher distance for the operating frequency. Moreover, while power output takes place just at the highest point in Fig. 5(b), the associated efficiency in Fig 5(a) becomes approximately 50 percent.

(a)

(b)
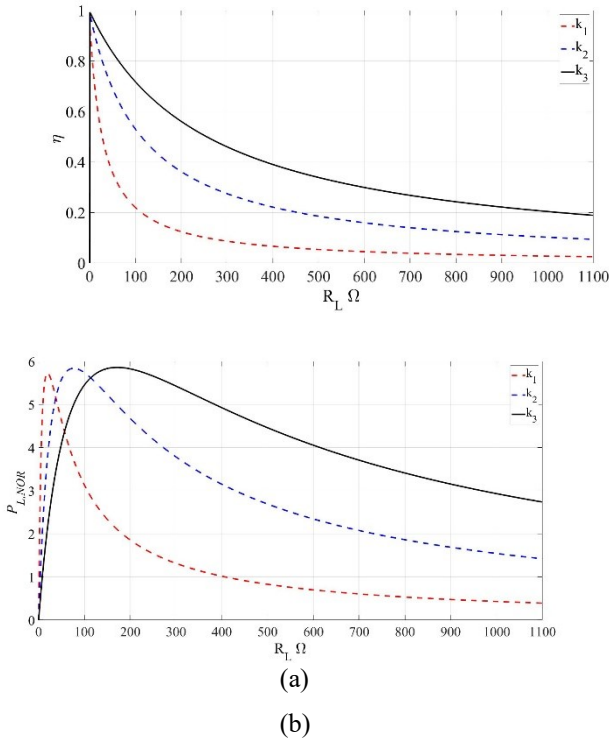
Fig. 6. (a) System efficiency versus various R_L (b) Normalized load power versus various R_L

The effectiveness of the process and load power against different loads for three distinct coupling coefficients is indicated in Fig. 6. It is shown by the Fig. 6(a) the efficiency profiles raises drastically for the early part as well as slowly decline against loads. The highest efficiency point appears while R_L is 3.28 Ω, for k = 0.25, similarly for R_L = 1.64Ω (while k = 0.17) as well as R_L = 0.32Ω (while k = 0.08). As observed from Fig.6(b) the load power profiles have an identical pattern to the efficiency waveforms, while k = 0.08,

the load power comes to the highest level when R_L becomes 4.6Ω, as well as the peak power value swings towards right when coupling coefficient rises as shown by Fig. 6(b).

III. SIMULATION AND DISCUSSION

Fig. 1 illustrates a conventional WPT structure based on a transmitting side coil and a receiving side coil are formed for simulating validation for estimation of highest possible overall efficiency as well as highest load power against various loading criteria and frequency as shown in the form of 3D graph in Fig. 8.

A. Varying frequency criteria

As per the Fig. 8. (a),(b),(c) for the k_1,k_2,k_3 coupling coefficient are shows at the lower load resistance, the frequency split occur near the resonance frequency in the series resonance coil. And this can not appear when the coupling coefficient approaches zero. At the resonance frequency 85 kHz the system transfer highest power at the load side at lower coupling coefficient but the overall efficiency of the system will reduce. Moreover, to transfer the power at good efficiency we need to choose the alternative option with deferent coupling coefficient such as k=0.25. Indeed, the efficiency of the system with respect to normalize frequency at constant load R_L=6.35 Ω and k=0.25 is 97% as shown in figure 8(c) The highest performance has been appeared for f = 85 kHz though predicted, that is exactly the operating frequency of the simulated study. In fig. 8, the simulated efficiency profile corresponds to the theoretical efficiency pattern. Mostly due to the ohmic losses in the AC-DC converter and cables, some irregularity appears.

The peak load power values appears for f_1 and f_2 are 81802 Hz and 88647 Hz respectively, due to the frequency bifurcation concepts between transmitter and receiver coils inside a small range. The normalized load power estimated around the resonance frequency decreases by about 73%., 91% and 97% at k_1,k_2 and k_3 respectively are shown in figure 5(b). It shows that, the output power will be higher at low coupling. Thus the power output could be enhanced by setting the power amplifier operating frequency in a higher coupling zone, however, the overall efficiency has been no longer at its highest level.

B. Varying the coupling between the coils

Fig. 8 illustrates system normalized load power simulation findings with respect to frequencies and load resistances by varying the coupling between the transmitter and receiver coils. From Fig. 8(a)-(c), for the coupling coefficient k_1,k_2,k_3 the obtained load power are higher at the low coupling coefficient w.r.t low load resistance. But in series resonating case the low coupling coil have higher load power at normal load and the efficiency of system is lower. It will gradually increase and then decrease slowly as the load resistance are varying. The variation of load resistance is 0 Ω to 1100 Ω are chosen for analysis and understanding the behaviour of the system. In the series resonating condition, it's also shows that the load power will be approximate four times of normal

power at the resonating frequency together with the normal load resistance.

From Fig. 8(d), shows all the figures 8(a)-(c) together to correlate all the graph and their effects. Its shows that at the lower resistive load the frequency split occurs and it makes system become unstable. Moreover, we can get the information that we must operate resonating coil at particular load resistance to overcome the frequency split. Apart from that it also shows that, at the normal load condition along with the different coupling coefficients such as k_1, k_2, and k_3 the normalized power will be high and low at the lower and high coupling coefficient such as k_1 and k_3, and respectively the efficiency of the system lower and higher respectively.

C. Varying output resistance criteria

A comparative analysis of the system normalized load power computed and simulated against different loads can be seen in Fig. 8 while operating frequency is 85 KHz, as well as coupling coefficient, k_1, k_2, and k_3 are 0.08, 0.17 and 0.25 respectively. From Fig. 8(a), near the starting while k_1=0.08, normalized load power rises drastically; the highest level attains (5.724) while R_L is 18.7Ω. The power is dropped significantly or even decreased to 25% once R_L becomes 100 Ω. As can be observed from Fig. 8(b), the normalized load power at k_2=0.17, achieves its highest level when the load becomes 77Ω as well as reduces steadily with increasing loads. Once load becomes more than 100Ω, the load power falls up to 35%. From Fig. 8(c), the normalized load power reaches the maximum (5.8603) at R_L=173 Ω and after that, the power is declined steadily with increasing loads while k_3=0.25.

The combined analysis of system normalized power against different loads in Fig. 8(a)-(c) are plotted in Fig. 8(d) to visualize all the figures and their comparative impacts. The range of load resistance is from 0-1100 ohms. In the series resonating condition, plots depict that the load power will be about four times the normal power at the resonating frequency with the normal load resistance, even though the load resistance is the same as before. Apart from that it also
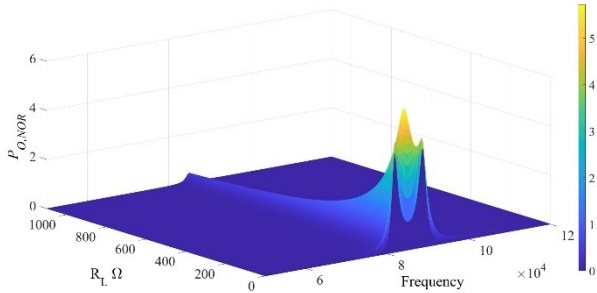
shows that load power comes to the highest level when R_L becomes low, as well as the peak power point swings towards the right when the coupling factor rises from k_1 to k_2 and k_3.

(a)

(b)
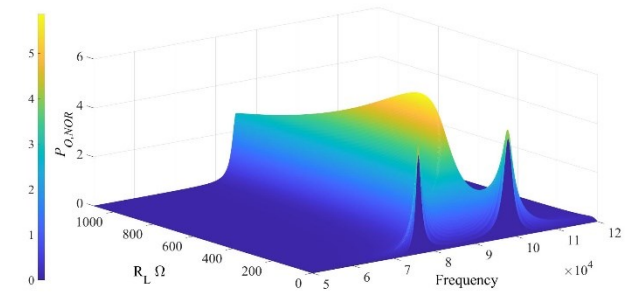
(c)
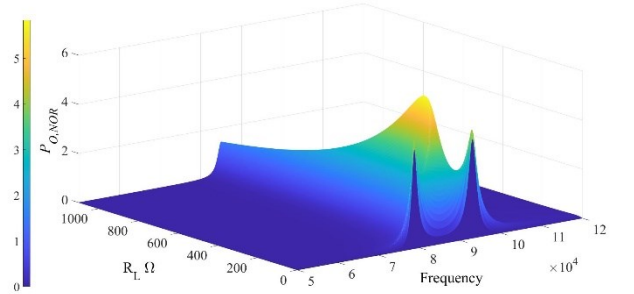
(d)

Fig. 7. (a) System Normalized Load Power as a function of various R_L and frequencies at k_1 (b) System Normalized Load Power as a function of various R_L and frequencies at k_2 (c) System Normalized Load Power as a function of various R_L and frequencies at k_3 (d) System Normalized Load Power as a function of various R_L and frequencies at k_1, k_2 and k_3

IV. CONCLUSION

This work focuses on the study and analyses for the optimal performnce and highest load power based on the two-winding WPT technology against various coil separations,
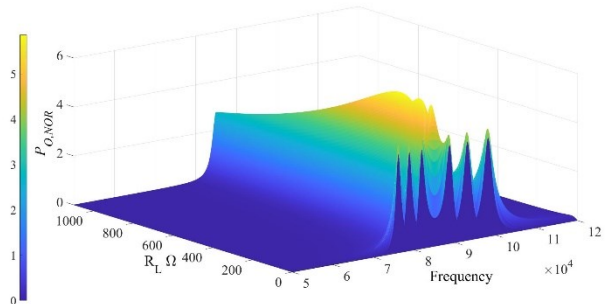
frequencies and load characteristics with the help of MATLAB/Simulation. The highest system efficiency often occurs at the operating frequency as from the results of the simulation, when the optimal load power is attained at the bifurcated frequency. Altering the load resistance could even enhance system efficiency as well as power output as a comparison to adjustable frequency scenarios. As the prototype development and enhancement of the ICPT system, the measurement of the highest system efficiency along with the highest load power is essential. The appropriate operating frequency and optimal load resistance can be selected to optimize system performance or to maximize load power against various working scenarios. Simulated study results validate the analytical observations and design methodologies in terms of obtaining overall efficiency maximization and highest load power. We will implement this methodology in

our future work for the experimental prototype development and improvement of the WPT system.

REFERENCES

[1] T. Ma and O. A. Mohammed, "Optimal charging of plug-in electric vehicles for a car-park infrastructure", IEEE Trans. Ind. Appl., vol. 50, no. 4, pp. 2323-2330, Jul./Aug. 2014.

[2] Global EV Outlook, 2019, [online] Available: https://www.iea.org/publications/reports/globalevoutlook2019/.

[3] M. O. Badawy et al., "Design and implementation of a 75-kW mobile charging system for electric vehicles", IEEE Trans. Ind. Appl., vol. 52, no. 1, pp. 369-377, Jan./Feb. 2016.

[4] A. Ahmad, M. S. Alam and R. Chabaan, "A Comprehensive Review of Wireless Charging Technologies for Electric Vehicles," in IEEE Transactions on Transportation Electrification, vol. 4, no. 1, pp. 38- 63, March 2018.

[5] D. Patil, M. K. McDonough, J. M. Miller, B. Fahimi and P.T. Balsara, "Wireless Power Transfer for VehicularApplications: Overview and Challenges," in IEEE 3-37, Transactions on Transportation Electrification, vol. 4, no. 1, pp. March 2018.

[6] S. Li and C. Mi, "Wireless power transfer for electric vehicle applications," IEEE J. Emerg. Sel. Topics Power Electron., vol. 3, no. 1, pp. 4–17, Mar. 2015.

[7] C. Fernandez, O. Garcia, R. Prieto, J. A. Cobos, S. Gabriels, and G. Van Der Borght, "Design issues of a core-less transformer for a contact-less application," in Proc. Appl. Power Electron. Conf. Expo., Oct. 2002, pp. 339– 345.

[8] G. B. Joung and B. H. Cho, "An energy transmission system for an artificial heart using leakage inductance compensation of transcutaneous transformer," IEEE Trans. Power Electron., vol. 13, no. 6, pp. 1013–1022, Nov. 1998

[9] A. Ridge, K. K. Ahamad, R. McMahon and J. Miles, "Development of a 50 kW Wireless Power Transfer System," 2019 IEEE PELS Workshop on Emerging Technologies: Wireless Power Transfer (WoW), 2019, pp. 406-409, doi: 10.1109/WoW45936.2019.9030672.

[10] R. K. Jha, G. Buja, M. Bertoluzzo, S. Giacomuzzi and K. N. Mude, "Performance Comparison of the One-Element Resonant EV Wireless Battery Chargers," in IEEE Transactions on Industry Applications, vol. 54, no. 3, pp. 2471-2482, May-June 2018, doi: 10.1109/TIA.2018.2796058.

[11] L. Yongseok, T. Hoyoung, L. Seungok and P. Jongsun, "An Adaptive Impedance-Matching Network Based on a Novel Capacitor Matrix for Wireless Power Transfer," IEEE Trans. Power Electron, vol. 29, no. 8, pp. 4403-4413, Aug. 2014.

[12] C.-S. Wang, G. A. Covic and O. H. Stielau, "Power transfer capability and bifurcation phenomena of loosely coupled inductive power transfer systems", IEEE Trans. Ind. Electron., vol. 51, no. 1, pp. 148-157, Feb. 2004.

[13] Z. Pantic, B. Sanzhong and S. Lukic, "ZCS LCC-compensated resonant inverter for inductive-power-transfer application", IEEE Trans. Ind. Electron., vol. 58, no. 8, pp. 3500-3510, Aug. 2011.

[14] J2954 Wireless Power Transfer for Light-Duty Plug-In/Electric Vehicles and Alignment Methodology, 2017, [online] Available:https://www.sae.org/standards/content/j2954_201711/.